รายงานวิจัยฉบับสมบูรณ์

โครงการ การพัฒนาวัสดุและประยุกต์ใช้พอลิเมอร์นำไฟฟ้าเพื่อทำเป็นขั่วเคาเตอร์สำหรับเซลล์แสงอาทิตย์ชนิดสีย้อมไวแสง

Title Development of conductive polymer films as the counter electrode of dye-sensitized solar cell

โดย ผศ. ดร. สมัคร์ พิมานแพง และคณะ

สิงหาคม 2556

สัญญาเลขที่ MRG5480024

รายงานวิจัยฉบับสมบูรณ์

โครงการ การพัฒนาวัสดุและประยุกต์ใช้พอลิเมอร์นำไฟฟ้าเพื่อทำเป็นขั้วเคาเตอร์สำหรับเซลล์แสงอาทิตย์ชนิดสีย้อมไวแสง

Title Development of conductive polymer films as the counter electrode of dye-sensitized solar cell

ผู้วิจัย	สังกัด
1. ผศ. ดร.สมัคร์ พิมานแพง	ภาควิชาฟิสิกส์ มหาวิทยาลัยขอนแก่น
2. รศ. ดร.วิทยา อำมรกิจบำรุง	ภาควิชาฟิสิกส์ มหาวิทยาลัยขอนแก่น

สนับสนุนโดยสำนักงานคณะกรรมการการอุดมศึกษา สำนักงานกองทุนสนับสนุนการวิจัย และ มหาวิทยาลัยขอนแก่น

Content

บทคัดย่อ

รหัสโครงการ: MRG5480024

ชื่อโครงการ: การพัฒนาวัสดุและประยุกต์ใช้พอลิเมอร์นำไฟฟ้าเพื่อทำเป็นขั้วเคาเตอร์สำหรับเซลล์แสงอาทิตย์ชนิดสีย้อมไวแสง

ชื่อนักวิจัย และสถาบัน: ผศ. ดร.สมัคร์ พิมานแพง ภาควิชาฟิสิกส์ มหาวิทยาลัยขอนแก่น

อีเมล์: samukpi@kku.ac.th

ระยะเวลาโครงการ: 2 ปี

บทคัดย่อ:

ในงานวิจัยนี้ได้ทำการศึกษาและประดิษฐ์ขั้วเคาร์เตอร์ของเซลล์แสงอาทิตย์ชนิดสีย้อมไวแสงจากสารแคตตาลีส (catalyst) ต่างๆ เพื่อลดการใช้สารแพลทตินัม สารที่นำมาศึกษาในงานวิจัยนี้ได้แก่ multiwall carbon nanotubes (MWCNTs), polypyrrole, tungsten carbibe (WC), palladium (Pd) ผลการศึกษาพบว่าฟิล์ม MWCNTs เตรียมด้วยวิธี hydrothermal ให้ประสิทธิภาพสูงสุดเท่ากับ 7.66% ฟิล์ม MWCNTs-Pt เตรียมด้วย electrophoretic deposition ให้ประสิทธิภาพสูงสุดเท่ากับ 8.90% ฟิล์ม polypyrrole-MWCNTs เตรียมด้วย chemical deposition ให้ประสิทธิภาพสูงสุดเท่ากับ 6.56% ฟิล์ม WC-Pt ให้ประสิทธิภาพสูงสุดเท่ากับ 4.29% การที่ประสิทธิภาพแตกต่างกันเพราะว่าฟิล์มแต่ละชนิดมีค่าการนำไฟฟ้าและการเกิดปฏิกิริยาเคมีที่แตกต่างกัน

คำหลัก: เซลล์แสงอาทิตย์ชนิดสีย้อมไวแสง; ขั่วเคาร์เตอร์; แคตตาลีส

Abstract

Project Code: MRG5480024

Project Title: Development of conductive polymer films as the counter electrode of dye-sensitized solar cell

Investigator: Samuk Pimanpang

E-mail Address: samukpi@kku.ac.th

Project Period: 2 years

Abstract:

In this work, we had studied many catalysts (MWCNTs, polypyrrole, WC or Pd) for fabricating the dye-senstized solar cell (DSSC) counter electrode. The different efficiencies were obtained from each catalyst. The highest efficiency based on the annealed hydrothermal treatment MWCNTs (AHT-MWCNTs) DSSCs is 7.66%. The highest DSSC efficiency based on the composited Pt-MWCNTs prepared by electrophoretic method is 8.90%. The highest DSSC efficiency based on the composited polypyrrole-MWCNTs DSSCs is 6.56%. The highest DSSC efficiency based on the composited Pt-WC DSSCs using organic electrolyte is 4.29%. The highest efficiency of the inverted flexible DSSCs based on the organic electrolyte is 2.64%. The variation of the cell performances is attributed to the different electrode catalytic activity and charge-transfer resistivity.

Keywords: Dye-sensitized solar cell; Counter electrode; Catalyst

Dye-sensitized solar cell

Introduction

The increasing of pollution and the decreasing of oil reservation have attracted researchers to find an alternative energy resource, which do not cause the pollution to the environment. Various types of non-polluted energy resources, such as solar cell or fuel cell, have been considered for the possible future energy resources. Solar cell has received a strong interested for many years, but it is not widely used yet because the solar cell price is still expensive. Many types of solar cell such as amorphous Si, crystal Si, GaAs, multilayer solar cell or dye-sensitized solar cell, are fabricated. The dye-sensitized solar cell (DSSC) has been intensively studied because of its simple structure, low fabrication cost, promising light harvesting efficiency and environmental friendliness. The high energy conversion efficiency of dye-sensitized solar cells is accomplished through the use of a highly porous semiconductor film coated with a monolayer dye-sensitizer as the working electrode, which was developed by O'Regan and Grätzel in 1991 [1]. TiO_2 nanoparticles are commonly used as a semiconductor because they deliver the highest energy conversion efficiency among semiconductors (ZnO, Nb_2O_5, WO_3, In_2O_3, SnO_2) [2-5]. TiO_2 nanoparticles serve as the electron-transport medium between dye-sensitizers and the electron collector (transparent conductive substrate). Electrons from the electron collector will flow through the external load reaching the counter electrode, and undergo reduction with tri-iodide ($I_3^- + 2e^- \rightarrow 3I^-$) with the help of the catalyst film. Thus, the catalyst film (counter electrode) is an important component of the DSSC device, which directly affects the cell performance.

Platinum (Pt) film is commonly used as the DSSC counter electrode because of its good catalytic activity, but Pt is an expensive material. Other cheaper materials have been studied as an alternative DSSC catalyst such as carbon black, carbon nanotubes or conductive polymers [6-10]. Carbon nanotubes are considered for use as the DSSC counter electrode because of their unique properties such as good catalytic activity, good conductivity, high thermal stability, high aspect ratio and comparatively lower price than Pt. Conductive polymers are also interested in using as the counter electrode because of its easy fabrication, high redox reaction and also lower price than Pt. Thus, by switching to a carbon nanotube and conductive polymer counter electrode, the DSSC production costs should be minimized. However, at the present, the performance of the carbon nanotube and conductive polymer DSSCs is still poor. Therefore, the performance of the nanotube and polymer DSSCs is needed to be improved prior to a commercialize product.

Conductive polymers such as polyaniline, polypyrrole and PEDOT:PSS are successfully used as the film counter electrode. J.-G. Chen et. al. [11] used a spun PEDOT:PSS film and W. Hong et. al. [12] used spun graphene/PEDOT:PSS film coated on the conductive glass as the DSSC counter electrode, and they obtained a reasonable efficiency. W. Hong et. al. [12] found that the addition of graphene increases the solar cell performance. For polypyrrole and polyaniline, J. Wu et. al. [13] and Z. Li et. al. [14] had prepared polymer films by chemical deposition and electrochemical deposition on the conductive glass, respectively, and tested as the cell counter electrode. These two polymers provided a very promising DSSC efficiency. Chemical deposition will use chemicals to activate the polymerization onto the substrate. The disadvantage of this method is that it is hard to control the deposition

rate. Electrochemical deposition is used the voltage potential to activate the polymerization. The deposition rate will be controlled by the potential different. The electrochemical deposition can perform by two ways: 1) direct voltage and 2) cyclic voltage.

In this report, we had used many different materials such as carbon nanotubes (CNTs), polypyrrole, PEDOT:PSS, $NiSO_4$, tungsten carbinde (WC), Pd or Pt for fabricating the DSSC counter electrodes. The performance of each counter electrode will report in each section separately.

Results

1. Fabrication of multiwall carbon nanotubes (MWCNTs) by hydrothermal method for the DSSC counter electrodes

MWCNTs films

CNT films were coated on FTO (8 Ω/sq., Solarnix) by a hydrothermal method (PARR 5500 series compact reactor). Optical and scanning electron microscope (SEM) images of hydrothermally deposited CNT (HT-CNT) film are presented in Fig. 1(a). The optical image shows CNT coating onto FTO substrate. The SEM image, Fig. 1(a), reveals non-uniform CNT deposition with impurities. Impurities were likely generated by CNT decomposition during acid treatment and/or hydrothermal process. They can also arise from CVD preparation. CNTs bond to FTO glass through functional group interaction as illustrated in Fig. 1(c).

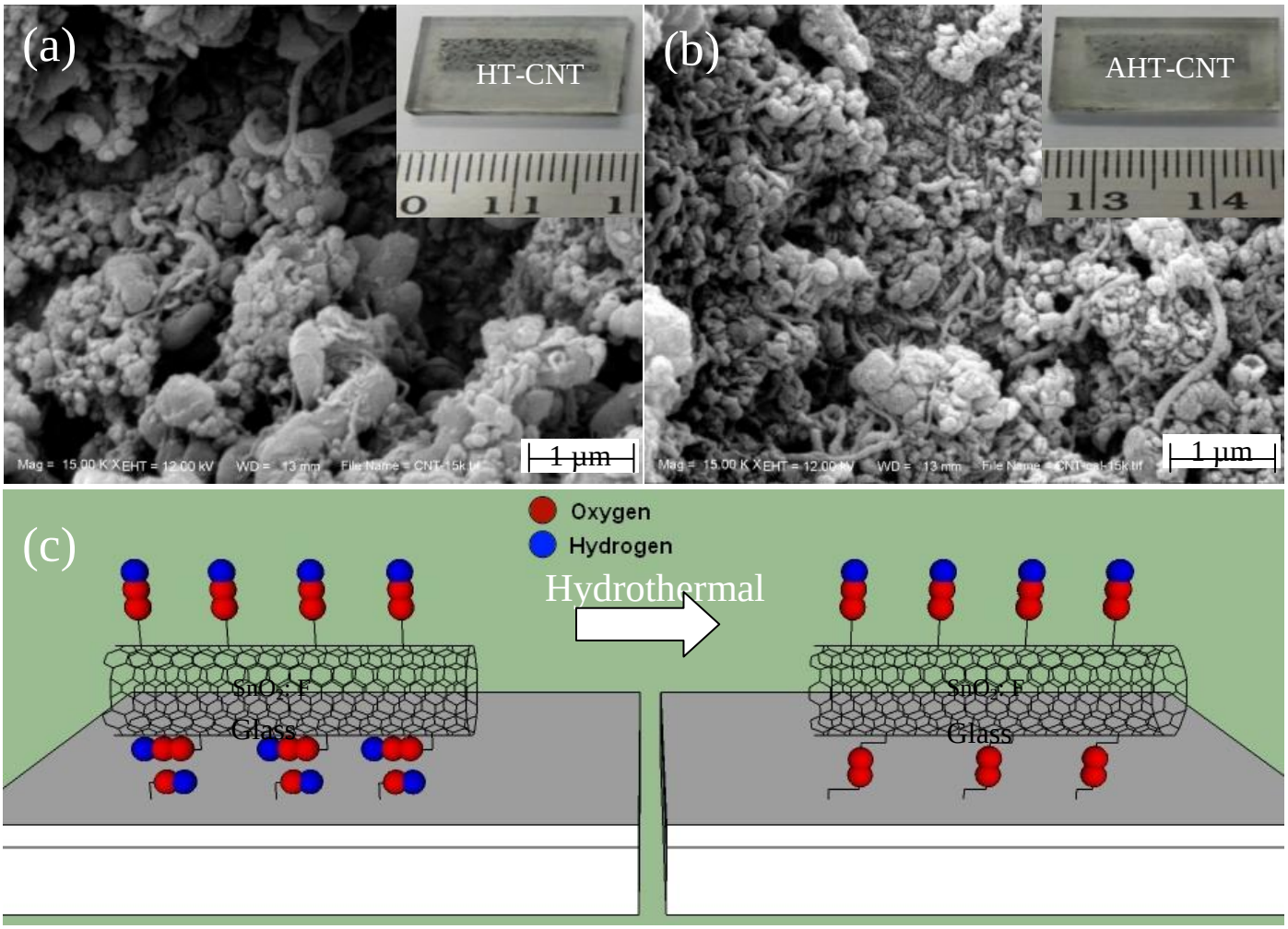

Fig. 1: (a) Optical and SEM images of HT-CNT, (b) optical and SEM images of AHT-CNT, and (c) schematic presenting the functional groups of CNTs and FTO interaction.

Solar cell efficiency

DSSCs were assembled using dye-sensitizer coated TiO_2 films as working electrodes (WEs) and HT-CNT films as CEs. Carbon film was removed to maintain an active area of 1.5 cm x 0.3 cm as shown in optical image, Fig. 1(a). Cell performance was measured using a solar simulator (PEC-L11, Japan) under light intensity of 100 mW/cm^2. The photocurrent-density (J) vs. photovoltage (V) curves are shown in Fig. 2. Photoelectric parameters such as short-circuit current density (J_{sc}), open-circuit voltage (V_{oc}), fill factor (FF) and energy conversion efficiency (η) were extracted from J-V curves and are summarized in Table I. It is seen that FF and η of HT-CNT DSSC (0.21 and 2.37%) are much lower than those of sputtered-Pt DSSC (0.73 and 8.01%). Since the WEs and electrolyte of these two devices were fabricated using the same conditions, the factors impacting performance differences should be from the CEs. Surprisingly, cell performance is significantly improved to 7.66% after film annealing. The η enhancement is subjected to the increment of FF from 0.21 to 0.68.

Table 1: Summary of open-circuit voltage (V_{oc}), short-circuit current density (J_{sc}), fill factor (FF) and solar cell efficiency (η) of hydrothermal treatment carbon nanotube (HT-CNT), annealed hydrothermal treatment carbon nanotube (AHT-CNT) and Pt DSSCs. I_D/I_G values of HT-CNT and AHT-CNT.

Electrode	J-V				Raman
	J_{sc} (mA.cm^{-2})	V_{oc} (V)	FF	η (%)	I_D / I_G
HT-CNT	14.40	0.79	0.21	2.37	1.17
AHT-CNT	14.27	0.78	0.68	7.66	0.97
Pt	14.02	0.77	0.73	8.01	N/A

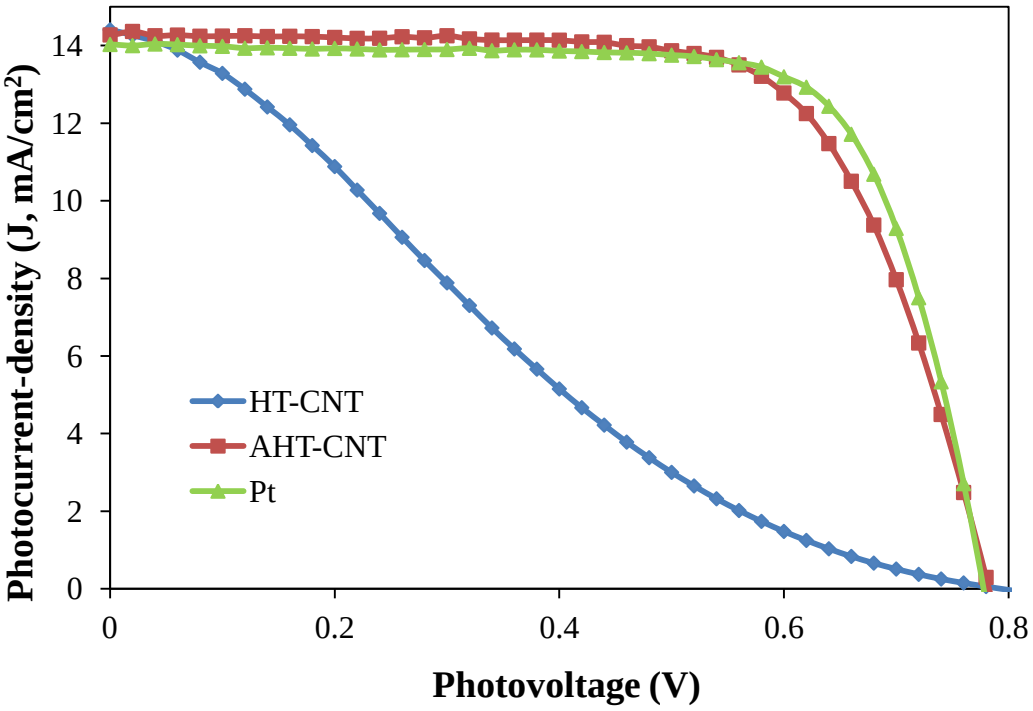

Fig. 2: Photocurrent-density (J) vs. photovoltage (V) curves of HT-CNT, AHT-CNT and Pt DSSCs.

2. Fabrication of mixed Pt and carbon nanotube films by the electrophoretic deposition for the DSSC counter electrodes

SEM images of counter electrodes

Fig. 3a shows the schematic electrophoretic deposition. Fig. 3b shows the curves of deposition current vs. time of MWCNTs, Pt and MWCNTs/Pt films. It appears that the current of Pt and MWCNTs/Pt films is higher than that of MWCNTs film. This implies faster coating or ion exchange at the electrode for Pt and composited MWCNTs/Pt films than for that of MWCNT film. This is due to the purity of Pt ions undergoing electrodeposition; however MWCNTs undergo electrophoretic deposition. Pure modified MWCNTs were attracted to the FTO surface because its surface was covered by negatively charge functional groups (-COOH or –OH), which were generated by acid modification. The presence of negative charges on nanotube surfaces is confirmed by nanotube coating on the positive electrode (anode). The interaction between modified nanotubes and FTO glass could occur via functional groups, -COOH group on MWCNTs with -OH group on FTO. In contrast, it is hypothesized that Pt and composited MWCNTs/Pt films were formed on the negative electrode (cathode). The opposite Pt deposition direction would be because the complex Pt ion ($Pt(NH_3)_4^{2+}$) is positively charged. Pt formation on FTO can be explained by following equations:

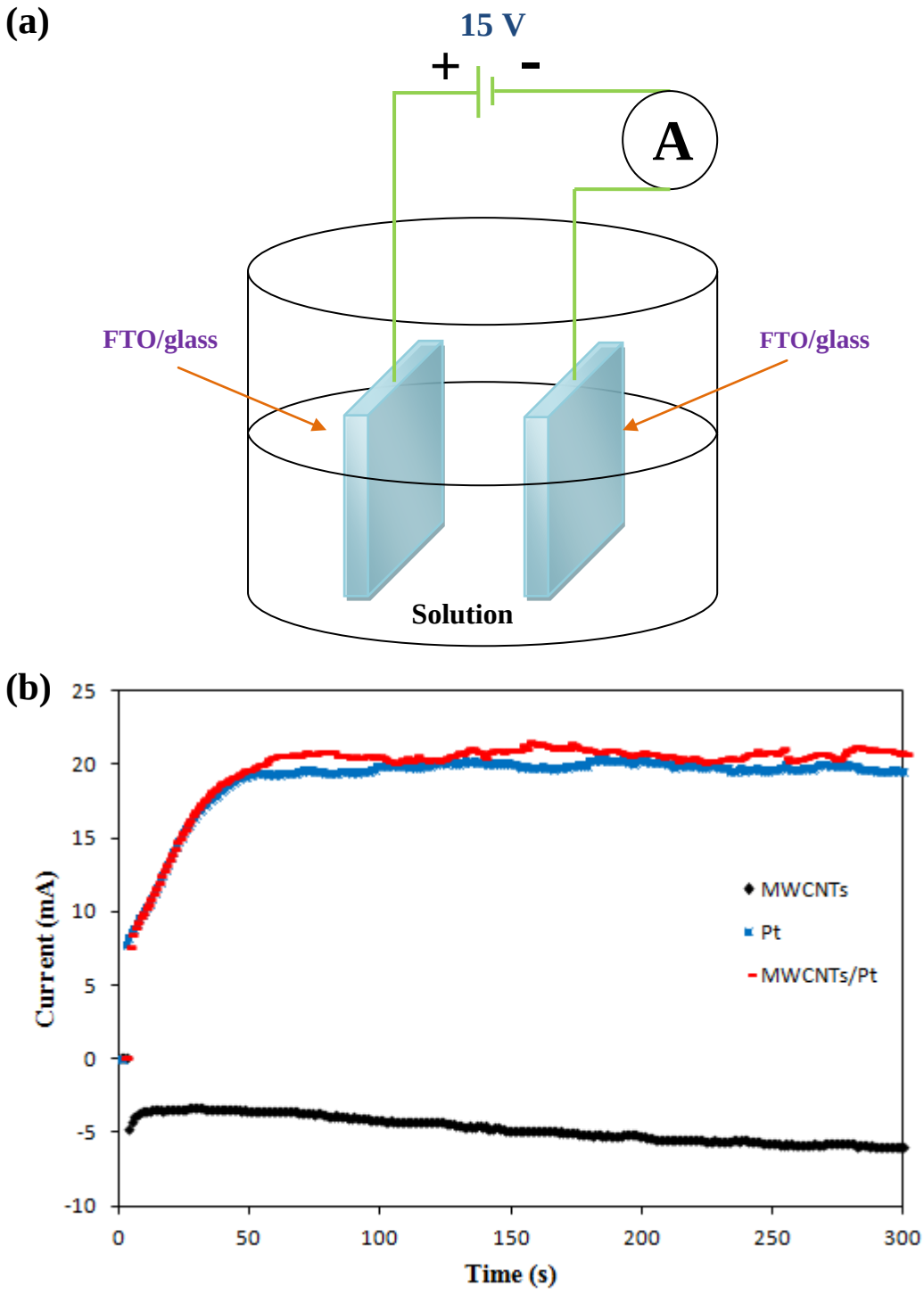

Fig. 3: (a) Schematic of the deposition setup and (b) the deposition current (I) vs. time (t).

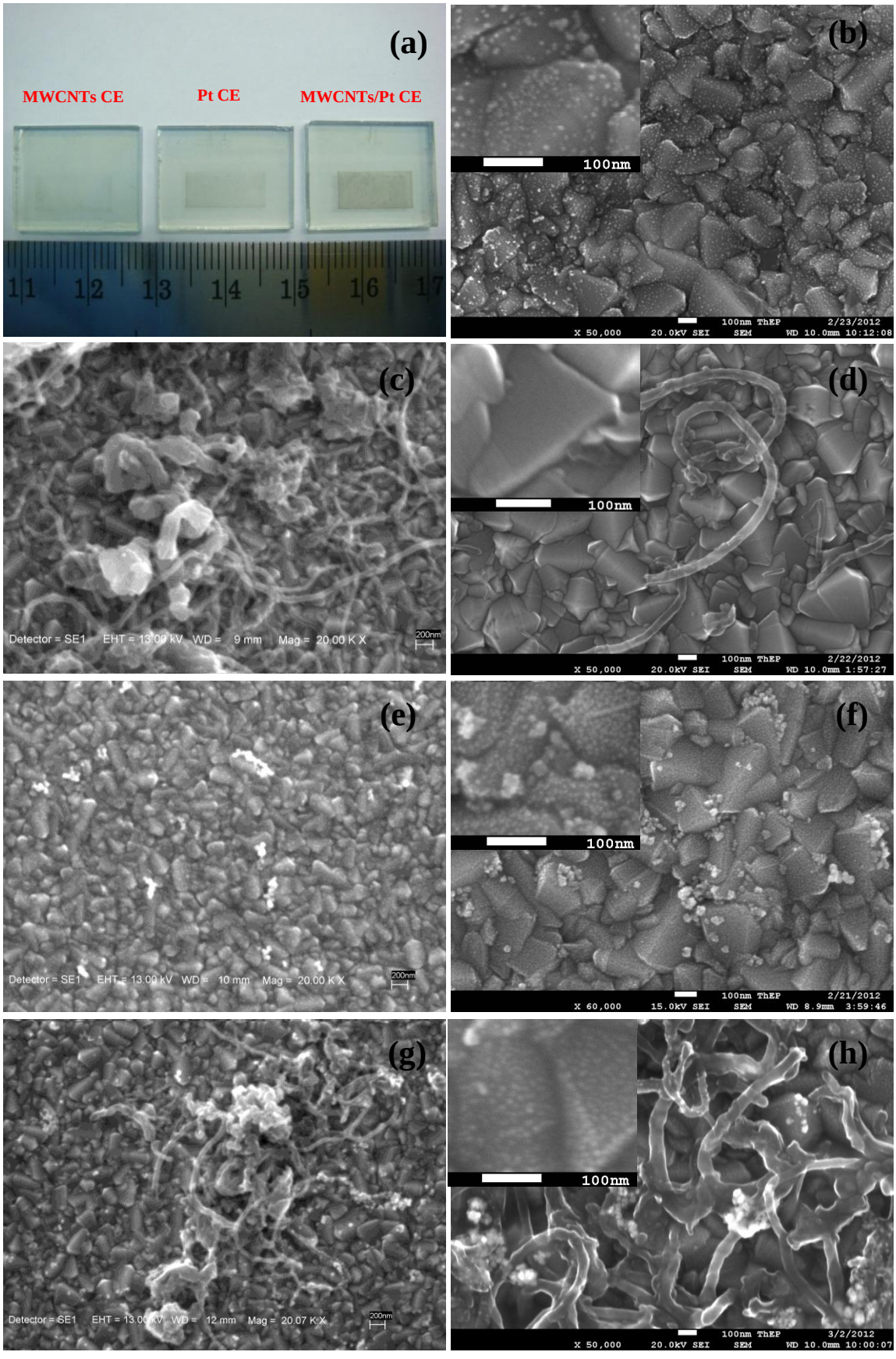
(a)
MWCNTs CE
Pt CE
MWCNTs/Pt CE
(b)
100nm
X 50,000 20.0kV SEI SEM 100nm ThEP WD 10.0mm 2/23/2012 10:12:08
(c)
Detector = SE1 EHT = 13.00 kV WD = 9 mm Mag = 20.00 K X 200nm
(d)
100nm
X 50,000 20.0kV SEI SEM 100nm ThEP WD 10.0mm 2/22/2012 1:57:27
(e)
Detector = SE1 EHT = 13.00 kV WD = 10 mm Mag = 20.00 K X 200nm
(f)
100nm
X 60,000 15.0kV SEI SEM 100nm ThEP WD 8.9mm 2/21/2012 3:59:46
(g)
Detector = SE1 EHT = 13.00 kV WD = 12 mm Mag = 20.07 K X 200nm
(h)
100nm
X 50,000 20.0kV SEI SEM 100nm ThEP WD 10.0mm 3/2/2012 10:00:07

Fig. 4: Photographs of MWCNTS(left), Pt(middle) and MWCNTs/Pt(right) films (a), low and high magnification SEM images of MWCNTs films (b, c), Pt films (d, e) and MWCNTs/Pt films (f, g) on FTO/glass substrates.

$$Pt(NH_3)_4Cl_2 \rightarrow Pt(NH_3)_4^{2+} + 2Cl^- \quad (1)$$

$$Pt(NH_3)_4^{2+} + 2e^- \rightarrow Pt^0 + 4NH_3 \quad (2)$$

Following this reasoning, during MWCNTs/Pt film deposition, MWCNTs were surrounded by $Pt(NH_3)_4^{2+}$ ions and were attracted to the negative FTO glass resulting in both MWCNTs and Pt deposition. In this case, MWCNTs are linked to conductive glass through Pt islands. Fig. 4a shows a photograph of MWCNTs (left), Pt (middle) and MWCNTs/Pt (right) counter electrodes. All films have black color, and MWCTs/Pt film has the darkest color. This is attributed to both Pt and nanotube formation. Figs. 4b, 4d and 4f show the top view SEM images of MWCNTs, Pt and MWCNTs/Pt on the FTO/glass substrates, respectively. High magnification FESEM image of MWCNTs film (Fig. 4c) detects nanotubes (diameter ~30-50 nm) coated on FTO surface. Pt islands are clearly observed on the Pt film (Fig. 4e).

DSSC performances

Fig. 5 shows the photocurrent-voltage curves of MWCNTs, Pt and MWCNTs/Pt DSSCs. Photoelectric parameters such as short-circuit current density (J_{sc}), open-circuit voltage (V_{oc}), fill factor (FF) and efficiency (η) were extracted from J-V curves and are presented in Table 2. The short-circuit current density (J_{sc}) and open-circuit voltage (V_{oc}) of Pt DSSC are about 14.28 mA/cm^2 and 0.79 V, compared to the J_{sc} of 16.10 mA/cm^2 and V_{oc} of 0.77 V of MWCNTs/Pt DSSC. The increase of J_{sc} leads to an improvement of MWCNT/Pt DSSC efficiency to 8.90%, which is higher than of Pt DSSC (~8.13%). For a comparison, a thermally deposited Pt electrode was fabricated and tested as a DSSC counter electrode. The DSSC with thermally deposited Pt counter electrode generates an efficiency of ~7.77%. We elected not to show its J-V curve to avoid confusion. This thermally deposited Pt DSSC efficiency is lower than those of the electrophoretic Pt and MWCNTs/Pt DSSCs. Comparing the performance of the Pt and MWCNTs/Pt DSSCs to values reported in the literature, the efficiency of the electrodeposited Pt DSSCs was ~6.40-7.6% and the efficiency of thermal deposited Pt DSSCs was ~5.58-6.3%. The electrophoretic deposition of the Pt and MWCNTs/Pt DSSCs in this work deliver better cell performance. The improvement of composited MWCNTs/Pt cell performance is mainly attributed to an increase in electrode effective surface area promoting electrode catalytic activity. MWCNTs DSSC provides the lowest FF (0.13), J_{sc} (12.82 mA/cm^2) and efficiency (1.42%). This is due to the low nanotube loading.

Table 2: Summary of series resistance (R_s), charge-transfer resistance at counter electrode/electrolyte (R_{ct1}), open-circuit voltage (V_{oc}), short-circuit current density (J_{sc}), fill factor (FF) and solar cell efficiency (η) of MWCNTs, Pt and MWCNTs/Pt DSSCs.

Counter electrode	R_s (Ohm)	R_{ct1} (Ohm)	J_{sc} (mA/cm^2)	V_{oc} (V)	FF	Efficiency (%)
MWCNT	~8.2	~1560	12.82	0.82	0.13	1.41 ± 0.20
Pt	~7.6	~1.9	14.28	0.79	0.72	8.13 ± 0.10
MWCNT/Pt	~7.9	~1.1	16.10	0.77	0.71	8.90 ± 0.30

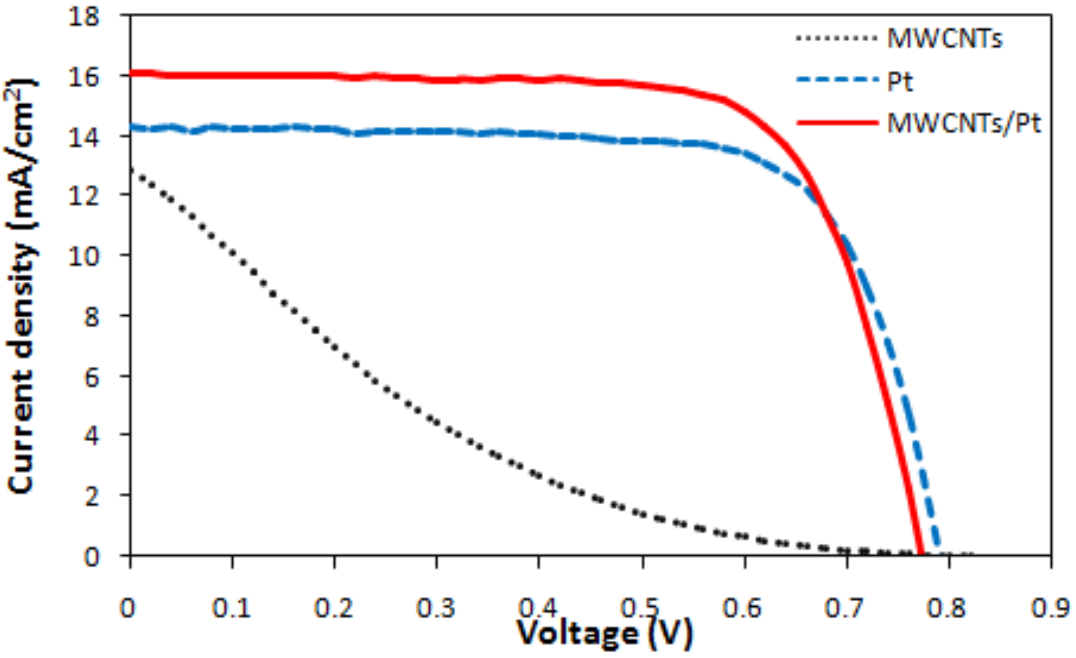

Fig. 5: Photocurrent density (J) vs. photovoltage (V) curves of MWCNTS, Pt and MWCNTs/Pt DSSCs.

3. Fabrication of polypyrrole and composited polypyrrole-nanoparticles (MWCNTs, Ni and TiO_2) for the DSSC counter electrodes

Film morphology

PPy films were successfully coated onto the FTO glass pieces by a chemical deposition method. Work pieces are shown in the optical and SEM images of Fig. 6. It was seen that the PPy and composited PPy-MWCNTs films had a black color. On the other hand, composited PPy-Ni and PPy-TiO_2 films were of a lighter color. This implies that more polymer was deposited in the PPy and composited PPy-MWCNTs films than in the composite PPy-Ni and PPy-TiO_2 films. The SEM image of pure PPy film, Fig. 6b, reveals nanoparticle formation with particle sizes ~380-460 nm. Polymer film did not fully cover the FTO substrate. Nanoparticle formations are also observed on all three composited PPy-nanoparticle films with particle sizes ~340-360 nm, as seen in Fig.6c-6e. Neither MWCNTs, Ni nor TiO_2 nanoparticles are detected on the composited films. This is likely due to the large polymer particles (~380-460 nm, Fig. 6b) covering smaller nanoparticles (~12-22 nm); i.e. nanoparticles were inserted in polymer particles.

DSSC performance

The performance of dye-sensitized solar cells was measured under an irradiation intensity of 100 mW/cm^2. Photocurrent-density (J) vs. photovoltage (V) curves are presented in Fig. 7. Photoelectric parameters such as short-circuit current density (J_{sc}), open-circuit voltage (V_{oc}), fill factor (FF) and energy conversion efficiency (η) were extracted from J-V curves. These parameters are listed in Table 3. It is seen that the efficiency of PPy-based DSSCs is increased after the combination of MWCNTs and Ni for both inorganic and organic electrolytes. They were slightly lower with TiO_2 addition. The efficiency of the T^-/T_2 based DSSCs is lower than the I^-/I_3^- based DSSCs for all cases. This is due to the lower J_{sc} and V_{oc}, as seen in Table 3. Composited PPy-MWCNTs DSSCs delivered the best performance among three composited cells. This is attributed to the high conductivity and good catalytic activity of MWCNTs. It is worth mentioning that the efficiency of the composited PPy-MWCNTs DSSC based on I^-/I_3^- electrolyte (~6.52%) in this work is lower than found by Peng et al. (~7.02%) [15]. This is possibly explained by incomplete polymer coating on the FTO substrate, as seen in Fig. 6. The chemically deposited PPy DSSCs (~6.00%) in this study generated higher cell efficiency than the electrochemically deposited PPy DSSCs (~4.72%) of our previous work [16]. Comparing cell performances with the Pt DSSCs, the efficiencies of the polymer and composited polymer-nanoparticle based DSSCs are slightly lower than Pt-based DSSCs for both electrolytes.

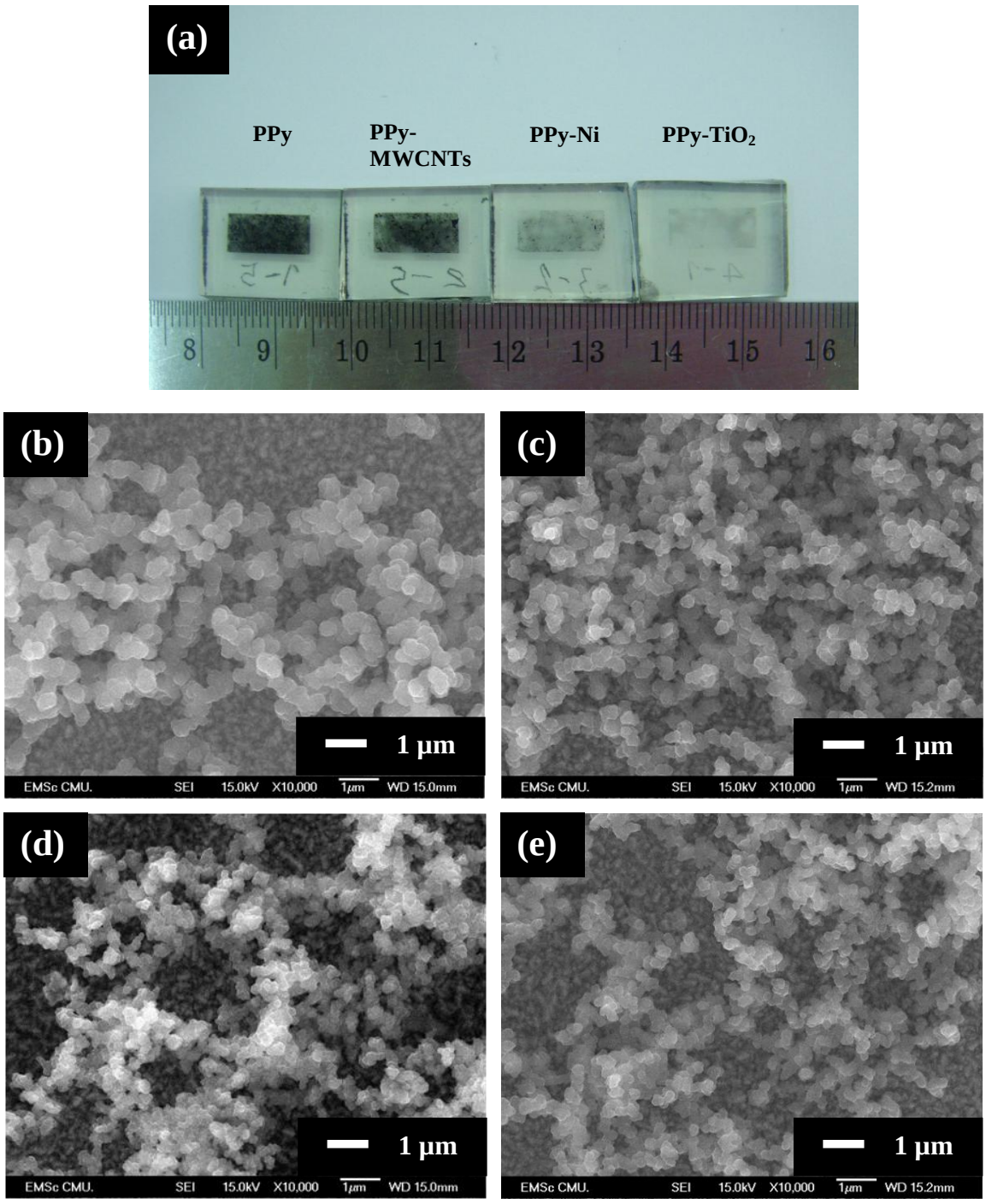

Fig. 6: (a) Optical image of PPy and composited PPy-nanoparticle films. SEM images of (b) PPy film, (c) PPy-MWCNTs film, (d) PPy-Ni film and (e) PPy-TiO_2 film.

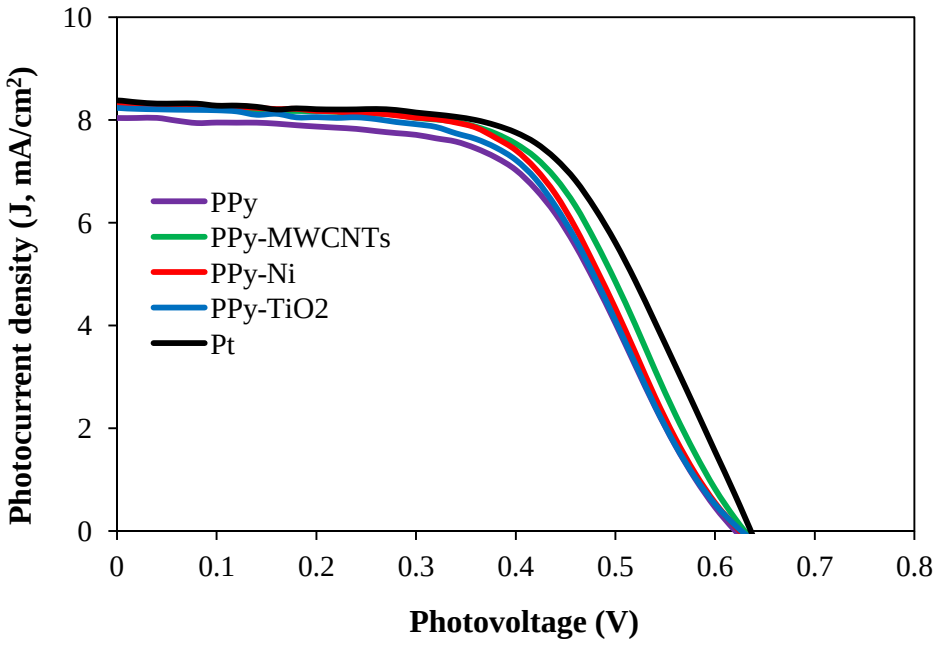

Fig. 7: Photocurrent-density (J) vs. photovoltage (V) curves of PPy, PPy-MWCNTs, PPy-Ni, PPy-TiO_2 and Pt DSSCs based on T^-/T_2 electrolyte.

Table 3: Summary of open-circuit voltage (V_{oc}), short-circuit current density (J_{sc}), fill factor (FF) and solar cell efficiency (η) of PPy, PPy-MWCNTs, PPy-Ni, PPy-TiO_2 and Pt DSSCs.

Electrode	J_{sc} (mA/cm^2)		V_{oc} (V)		FF		η (%)	
	I^-/I_3^-	T^-/T_2	I^-/I_3^-	T^-/T_2	I^-/I_3^-	T^-/T_2	I^-/I_3^-	T^-/T_2
PPy	13.65	8.04	0.71	0.62	0.62	0.56	6.00	2.81
PPy-MWCNTs	14.99	8.29	0.71	0.63	0.62	0.59	6.56	3.05
PPy-Ni	14.60	8.29	0.72	0.63	0.60	0.57	6.24	2.96
PPy-TiO_2	13.75	8.24	0.71	0.62	0.65	0.56	6.32	2.89
Pt	14.24	8.38	0.72	0.64	0.71	0.60	7.20	3.19

4. Fabrication of inverted flexible DSSCs

Film morphology

The optical image in Fig. 8(b) shows the formation of Pt films on conductive plastic for all four deposition durations. The film color becomes darker with increasing deposition time. This implies that more Pt particles formed on the plastic with increasing deposition time. The transparency of Pt films was analyzed using UV-visible spectroscopy. The film transmittance significantly decreased from ~84% to ~44% for the 30s-Pt film and the 120s-Pt film, respectively, as shown in Fig. 8(b). This is consistent with the darkening of film colors as seen in the optical image. FESEM was used to characterize the Pt structure. Figs. 9(a, c, e, g) reveal Pt nanoparticle formation with particle sizes ~1-5 nm on the conductive plastic of all four samples. The number of Pt islands increased with increasing deposition duration. The increase in the number of Pt islands is an explanation of the decrease in film transmittance. Energy Dispersive X-ray Spectroscopy (EDS) results, Figs. 9(b, d, f, h), show the Pt peak at ~2.1 eV. This confirms that nanoparticles formed on the plastic surfaces are Pt islands for all four samples.

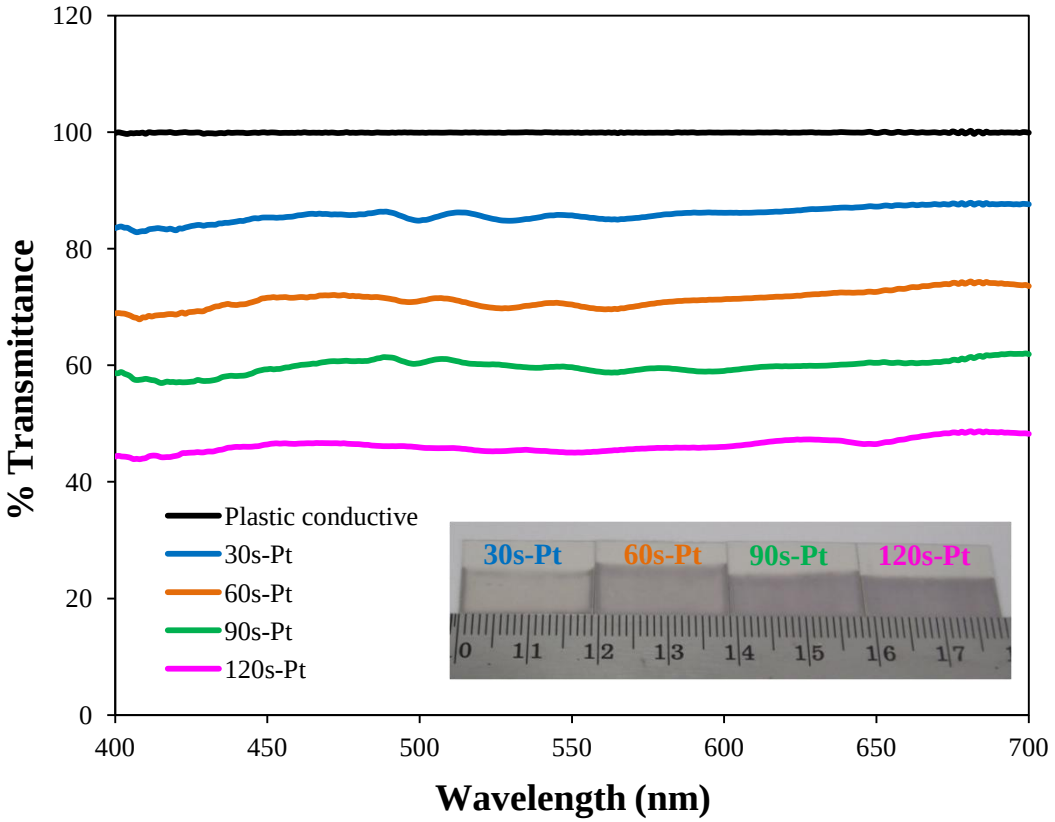

Fig. 8: The optical image and the percent transmittance of the Pt/plastic films reference with the conductive plastic.

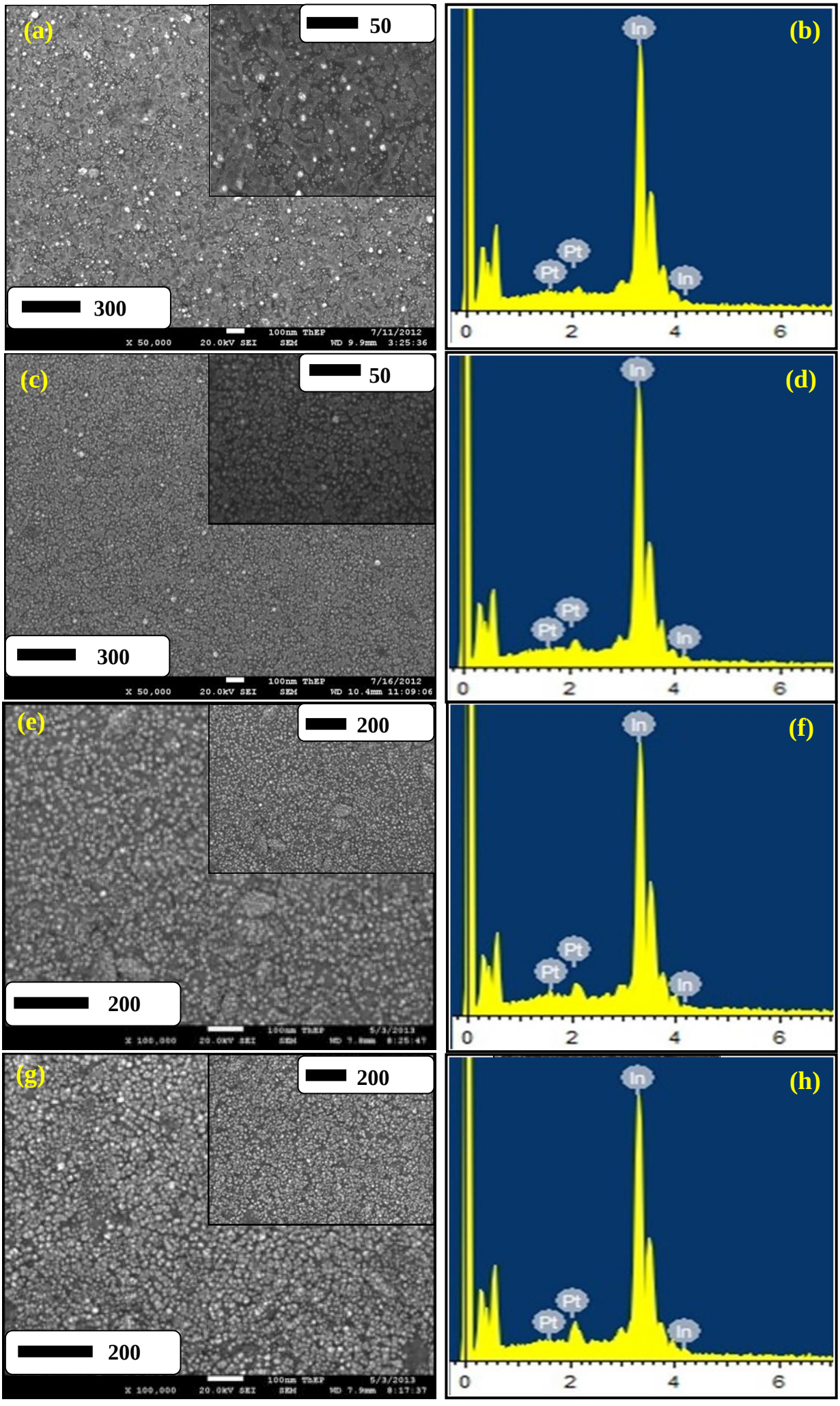
(a)
50
300
100nm ThEP 7/11/2012
X 50,000 20.0kV SEI SEM WD 9.9mm 3:25:36
(b)
In
Pt
Pt
In
0
2
4
6
(c)
50
300
100nm ThEP 7/16/2012
X 50,000 20.0kV SEI SEM WD 10.4mm 11:09:06
(d)
In
Pt
Pt
In
0
2
4
6
(e)
200
200
(f)
In
Pt
Pt
In
0
2
4
6
(g)
200
200
100nm ThEP 5/3/2013
X 100,000 20.0kV SEI SEM WD 7.9mm 8:17:37
(h)
In
Pt
Pt
In
0
2
4
6

Fig. 9: (a) FESEM image of the 30 sec-Pt film (30s-Pt) coated on the conductive plastic and (b) its EDS spectrum. (c) FESEM image of 60s-Pt film and (d) its EDS spectrum. (e) FESEM image of 90s-Pt film and (f) its EDS spectrum. (g) FESEM image of 120s-Pt film and (h) its EDS spectrum.

DSSC performance

Flexible dye-sensitized solar cells were assembled using electrodeposited-Pt/plastic as a counter electrode and TiO_2/SS as working electrode. Light was shined on the counter electrode and travelled through the counter electrode and the electrolyte to the working electrode. The photocurrent density (J) and photovoltage (V) was measured under 1 sun. J-V spectra (first DSSC of each Pt condition in Table 1) are shown in Fig. 5. DSSC parameters were extracted from the J-V curves and summarized in Table 1. It can be seen in Table 1 that the efficiency of the 30s-Pt DSSC is the highest ~2.72%, and that cell efficiency decreases with increasing Pt film thickness. Four cells were assembled and tested for each Pt condition. It sees that the J_{sc}, V_{oc}, FF and η values of each condition are slightly difference. This means that the property of the working electrode is almost controllable, which suggests the reproducing of the screening method. The average η value also exhibits the decreasing trend. Reduction of the cell efficiency was influenced by lowering of the short-circuit current density (J_{sc}), as seen in Fig. 5 and Table 1. J_{sc} is related to the current density produced by the solar cell (J_{ph}) as follows:

$$J_{sc} = J_{ph} - J_0\left(e^{\frac{q(J_{sc}\cdot A\cdot R_S)}{k_B T}} - 1\right) \qquad (3)$$

where, q is the electron charge, J_0 is a constant, A is the cell area, R_s is the cell series resistance, k_B is a Boltzman constant and T is temperature. From this equation, the decreasing of J_{ph} leads to the reducing of J_{sc}. J_{ph} is related to the incident light flux, $b_s(\lambda,x)$, as follows [14]:

$$J_{ph} = q\int_{\lambda=0}^{\lambda=\infty}\int_{x=0}^{x=d} T(\lambda)\cdot\eta(\lambda)\cdot\alpha(\lambda)\cdot b_s(\lambda,x)\cdot dx\cdot d\lambda \qquad (4)$$

where, $T(\lambda)$ is the probability of the photon transmission into the material, $\eta(\lambda)$ is the probability of the electron collected at the electron collector, $\alpha(\lambda)$ is the probability of photon adsorbed, x is the distance from the absorber surface, and d is the absorber thickness (TiO_2 film thickness). From eq. 2, it is seen that J_{ph} is directly dependent on the light flux, $b_s(\lambda,x)$, projected on the absorber (dye coated TiO_2 film).

In this inverted structure, light travels through the counter electrode and the electrolyte, as shown in Fig. 2(a). Thus, the light intensity focused on the TiO_2 surface is different for each Pt film. This is because Pt films have different transmittances as seen in Fig. 1(b). The light intensity focused on the TiO_2 surface (after some light was absorbed by the counter electrode and the electrolyte) can be roughly estimated from the transmittances of the Pt/plastic film and the electrolyte. The percent light transmittance through the counter electrode ($\%T_{CE}$) is determined directly from UV-visible spectra of Fig. 1(b). The percent light transmittance through the organic electrolyte ($\%T_{EL}$) is estimated from the UV-vis spectrum through the symmetric-conductive plastic cell spacing by parafilm (~150 μm) and filling with the organic electrolyte (conductive plastic‖organic electrolyte‖conductive plastic) referenced with the non-electrolyte cell (conductive plastic‖non-

electrolyte‖conductive plastic) in Fig. S3. At wavelength 530 nm, the percent light transmittance is ~93%. The wavelength at 530 nm was considered because dye N719 has its highest absorbance at this wavelength, as shown in Fig. S2. Thus, the percent light flux at wavelength 530 nm is only 78% (~0.84×0.93×100, $\%T_{CE}/100\times\%T_{EL}/100\times100$) of the incident light flux on the counter electrode projected on the TiO_2 film. The estimated percent light flux at wavelength 530 nm focused on the other three DSSCs is listed in Table 1. It is observed that the estimated light intensity projected on the TiO_2 film decreased from 78% to 42% for the 30s-Pt DSSC and the 120s-Pt DSSC, respectively. Therefore, the reduction of the light flux focused on the absorber is a primary factor that reduces DSSC short-circuit current density and cell efficiency.

Table 4: Summary of open-circuit voltage (V_{oc}), short-circuit current density (J_{sc}), fill factor (FF) and solar cell efficiency (η) of flexible DSSCs. The expected percent light flux at wavelength 530 nm of the incident light flux on the counter electrode projected on the TiO_2 film ($\%b_s$-TiO_2).

Electrode	J_{sc} ($mA\cdot cm^{-2}$)		V_{oc} (V)		FF		η (%)		Expected $\%b_s$-TiO_2 (at 530 nm)
	Cell	Average	Cell	Average	Cell	Average	Cell	Average	
30s-Pt	7.57 7.09 7.14 7.53	7.33 ± 0.25	0.62 0.62 0.61 0.61	0.62 ± 0.01	0.58 0.58 0.58 0.58	0.58 ± 0.01	2.72 2.56 2.58 2.69	2.64 ± 0.08	74
60s-Pt	7.10 5.90 6.39 6.87	6.57 ± 0.53	0.62 0.60 0.61 0.62	0.61 ± 0.01	0.58 0.60 0.59 0.61	0.60 ± 0.01	2.56 2.14 2.30 2.56	2.39 ± 0.21	65
90s-Pt	6.85 6.60 5.43 6.41	6.32 ± 0.62	0.60 0.61 0.60 0.60	0.60 ± 0.01	0.58 0.57 0.58 0.59	0.58 ± 0.01	2.40 2.30 1.91 2.28	2.22 ± 0.21	56
120s-Pt	5.80 6.50 5.96 5.81	6.02 ± 0.33	0.60 0.60 0.60 0.60	0.60 ± 0.00	0.58 0.56 0.57 0.58	0.57 ± 0.01	2.03 2.19 2.06 2.05	2.09 ± 0.07	42

5. Fabrication of mixed Pd-WC and Pt-WC by thermally deposited for DSSC counter electrodes

Film morphology

SEM image of WC film in Fig. 10(a) shows that WC particles are not fully covered the FTO surface. Particles seem to agglomerate forming big islands with the island size about 1-8 μm. Energy x-ray dispersive spectroscopy (EDS) of WC film in Fig. 10(b) contains the strong W and C peaks, implying that these islands are WC particles. SEM images of Pd and Pt films (in Fig. 10) compose of nanoparticles coated on FTO surface with the particle size of ~8 and ~12 nm for Pd and Pt films, respectively. Their EDS spectra, in Figs. 10(d) and 1(h), present the strong Pd and Pt peaks for the Pd and Pt films, respectively. This means that nanoparticles coated on the FTO surface are Pd and Pt. In case of mixed Pd-WC and Pt-WC films, SEM images in Figs. 10(e) and 1(i) present WC particles were decorated by nanoparticles. EDS spectra of Pd-WC (Fig. 10f) and Pt-WC (Fig. 10j) films confirm the achievement of mixing WC with Pd and WC with Pt.

DSSC performance

DSSCs were assembled using WC, Pd, Pd-WC, Pt and Pt-WC films as the counter electrodes. The cell performance was measured under an irradiation intensity of 100 mW/cm^2. Photocurrent-density (J) vs. photovoltage (V) curves are presented in Fig. 11. Photoelectric parameters such as short-circuit current density (J_{sc}), open-circuit voltage (V_{oc}), fill factor (FF) and energy conversion efficiency (η) were extracted from J-V curves and are listed in Table 5. It sees that the WC DSSC delivers the inferior efficiency (~0.78%). Interestingly, the composition of WC particles with other catalysts (Pd or Pt) greatly boosts up the cell efficiency to 4.62% for Pt-WC DSSC and to 3.85% for Pd-WC DSSC. The efficiency of the composited DSSCs is higher than those of the pure Pt DSSC (~3.85%) and Pd DSSC (~1.68%). The improved performance of the composited DSSCs is attributed to the good electrocatalytic activities. The reproducibility was tested by assembling three DSSC devices for each CE condition. Table 5 shows the performance of all fifteen DSSCs. It sees that the DSSC characteristics of each condition are quite closed. This means that the qualities of the working electrode, electrolyte and counter electrode are almost controllable.

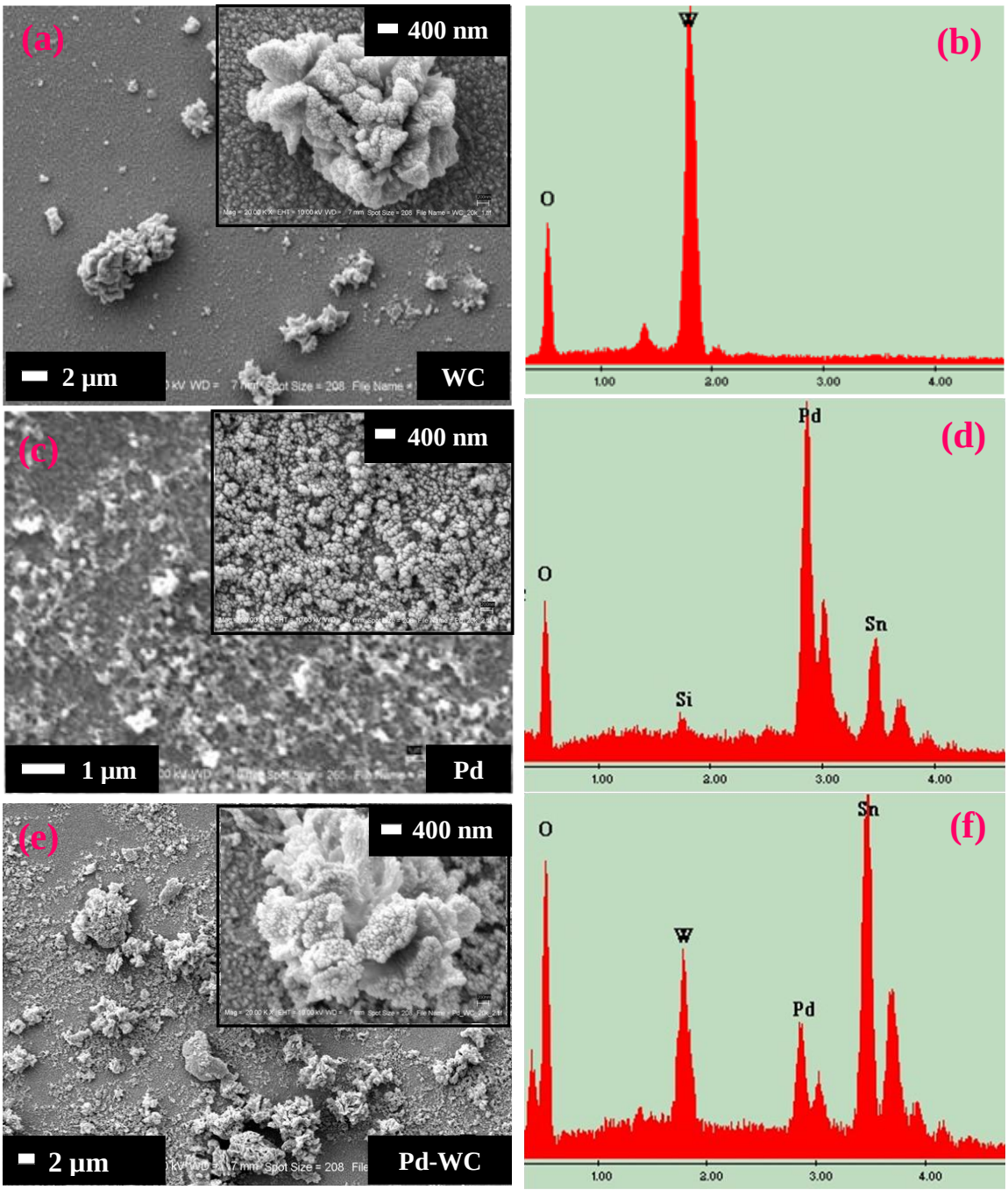
(a)
400 nm
2 µm
WC
(b)
W
O
1.00
2.00
3.00
4.00
(c)
400 nm
1 µm
Pd
(d)
Pd
O
Sn
Si
1.00
2.00
3.00
4.00
(e)
400 nm
2 µm
Pd-WC
(f)
Sn
O
W
Pd
1.00
2.00
3.00
4.00

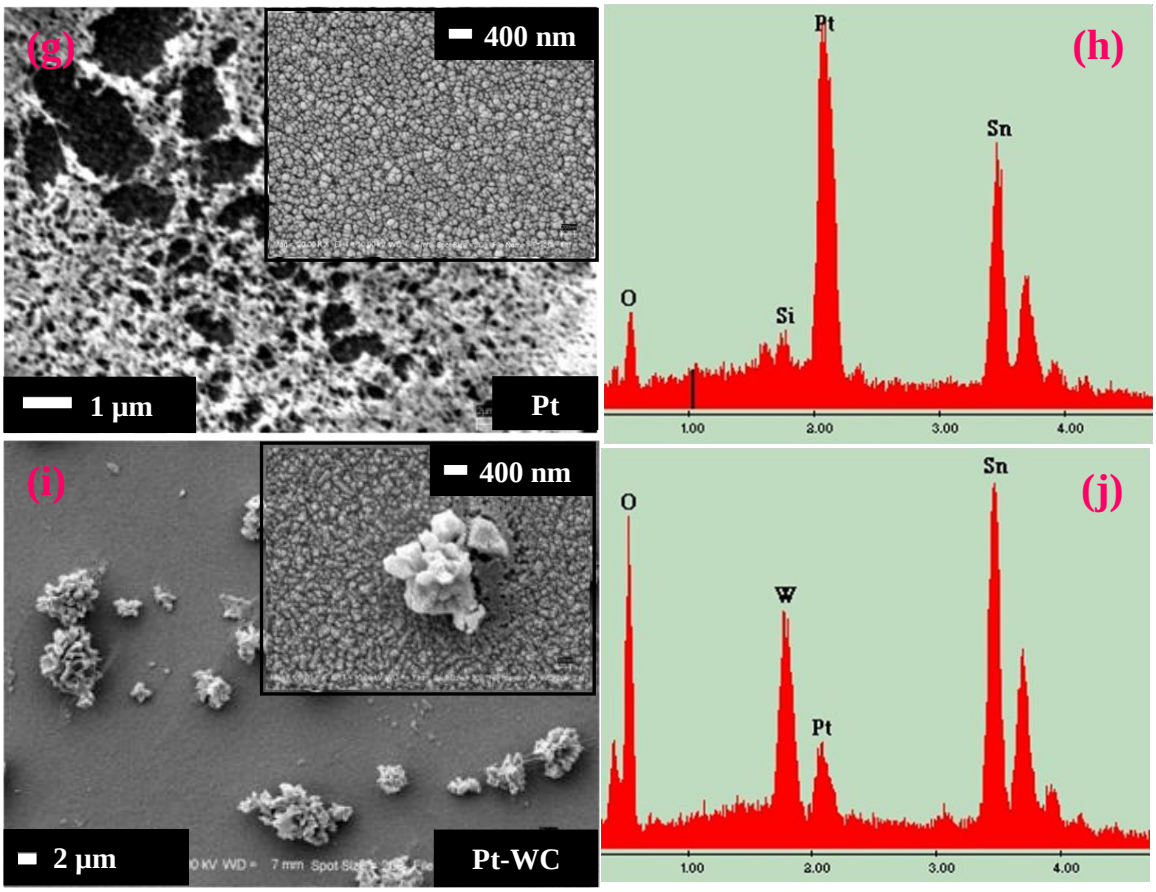

Fig. 10: (a) SEM image and (b) EDS spectrum of WC film. (c) SEM image and (d) EDS spectrum of Pd film. (e) SEM image and (f) EDS spectrum of Pd-WC film. (i) SEM image and (j) EDS spectrum of Pt-WC film.

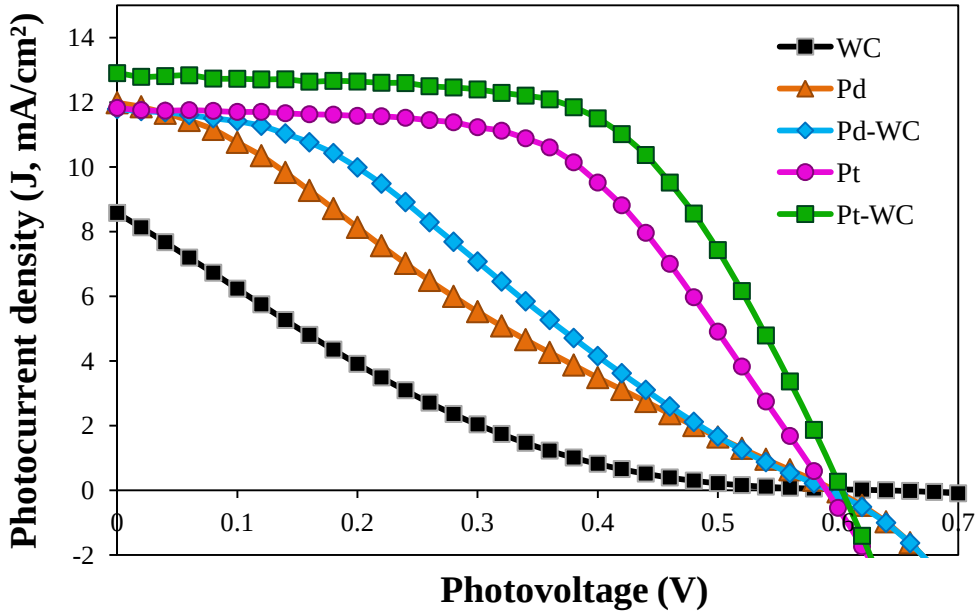

Fig. 11: Photocurrent-density (J) vs. photovoltage (V) curves of WC, Pd, Pd-WC, Pt and Pt-WC DSSCs based on the T^-/T_2 electrolyte.

Table 5: Summary of the solar cell characteristics of fifteen cells.

Counter Electrode	J_{sc} (mA·cm^{-2})		V_{oc} (V)		FF		η (%)	
	Cell	Average	Cell	Average	Cell	Average	Cell	Average
Pd	11.98 11.03 11.78	**11.60±0.50**	0.60 0.60 0.60	**0.60±0.00**	0.23 0.20 0.19	**0.21±0.02**	1.68 1.33 1.38	**1.46±0.19**
Pd-WC	11.79 10.85 11.10	**11.25±0.49**	0.59 0.60 0.60	**0.60±0.01**	0.31 0.33 0.25	**0.29±0.04**	2.15 2.19 1.69	**2.01±0.30**
Pt	11.82 11.45 10.96	**11.41±0.43**	0.59 0.61 0.61	**0.60±0.01**	0.55 0.55 0.56	**0.55±0.01**	3.85 3.81 3.74	**3.80±0.06**
Pt-WC	11.40 11.48 12.90	**11.93±0.84**	0.61 0.60 0.60	**0.60±0.01**	0.59 0.60 0.59	**0.59±0.01**	4.08 4.16 4.62	**4.29±2.99**
WC	8.65 8.57 8.93	**8.72±0.19**	0.64 0.64 0.64	**0.64±0.00**	0.13 0.14 0.13	**0.13±0.01**	0.70 0.78 0.75	**0.74±0.04**

Conclusion

The different cell performances were obtained from each catalyst. The highest efficiency based on the annealed hydrothermal treatment MWCNTs (AHT-MWCNTs) DSSCs is 7.66%. The highest DSSC efficiency based on the composited Pt-MWCNTs prepared by electrophoretic method is 8.90%. The highest DSSC efficiency based on the composited polypyrrole-MWCNTs DSSCs is 6.56%. The highest DSSC efficiency based on the composited Pt-WC DSSCs using organic electrolyte is 4.29%. The low charge-transfer resistance and the high electrode catalytic activity promote the cell performance. Therefore, the good catalyst for the I^-/I_3^- electrolyte should have high activity with I^-/I_3^- redox couple.

Future work

From this work, we found that the cheaper catalyst (MWCNTs, WC or polypyrrole) generate the promising efficiency as closed as to the Pt based DSSCs. However, its stability is still poor. We think that the solid state dye-sensitized solar cell should be a better solution even though it provides the lower efficiency. In future, we will use the knowledge on fabricating the working electrode (gained from this study) with the solid p-type materials such as CuI, CuSnS or $CsSnI_2$.

Acknowledgement

Author would like to thank mentors (Assit. Prof. Vittaya Amornkitbamrung) for the constructive suggestion and Madsakorn Towannang, Anongnad Thiangkaew, Wasan Maiaugree, Sumeth Siriroj, Khamsone Keothongkham, Phikun Ratphonsan, Wirat Jarernboon for help with the lab works. Authors would like to thank Intergrated Nanotechnology Research Center (INRC), Khon Kaen University for supplying the conductive glass and the conductive plastic. This work is supported by The Thailand Research Fund (TRF, MRG5480024), the Commission on Higher Education (CHE), and Khon Kaen University.

References

[1] B. O'Regan, M. Grätzel, Nature 353 (1991) 737-740.

[2] M. Grätzel, J. Photochem. Photobiol. A 164 (2004) 3-14.

[3] K. Tennakone, G.R.R. Kumara, I.R.M. Kottegoda, V.S.P. Perera, Chem. Commun. 1 (1999) 15-16.

[4] K. Sayama, H. Sugihara, H. Arakawa, Chem. Mater. 10 (1998) 3825-3832.

[5] Y. Fukai, Y. Kondo, S. Mori, E. Suzuki, Electrochem. Commun. 9 (2007) 1439-1443.

[6] A. Kay, M. Grätzel, Sol. Energy. Mater. Sol. Cell 44 (1996) 99-117.

[7] K. Imoto, K. Takahashi, T. Yamaguchi, T. Komura, J. Nakamura, K. Murata, Sol. Energy. Mater. Sol. Cell 79 (2003) 459-469.

[8] T.N. Murakami, M. Grätzel, Inorg. Chim. Acta 361 (2008) 572-580.

[9] K. Suzuki, M. Yamamoto, M. Kumagai, S. Yanagida, Chem. Lett. 32 (2003) 28-29.

[10] P. Balraju, M. Kumar, M.S. Roy, G.D. Sharma, Synthetic Met. 159 (2009) 1325–1331.

[11] J.-G. Chen, H.-Y. Wei, K.-C. Ho, Sol. Energy. Mater. Sol. Cell 91 (2007) 1472–1477.

[12] W. Hong, Y. Xu, G. Lu, C. Li, G. Shi, Electrochem. Commun. 10 (2008) 1555–1558.

[13] J. Wu, Q. Li, L. Fan, Z. Lan, P. Li, J. Lin, S. Hao, J. Pow. Sour. 181 (2008) 172–176.

[14] Z. Li, B. Ye, X. Hu, X. Ma, X Zhang, Y. Deng, Electrochem. Commun. 11 (2009) 1768–1771.

[15] S. Peng, Y. Wu, P. Zhu, V. Thavasi, S.G. Mhaisalkar, S. Ramakrishna, Journal of Photochemistry and Photobiology A: Chemistry 223 (2011) 97-102.

[16] K. Keothongkham, S. Pimanpang, W. Maiaugree, S. Saekow, W. Jarernboon, V. Amornkitbamrung, International Journal of Photoenergy, (2012) doi:10.1155/2012 /671326.

Output

Papers:

1. Madsakorn Towannang, **Samuk Pimanpang**, Anongnad Thiangkaew, Phikun Rutphonsan, Wasan Maiaugree, Viyada Harnchana, Wirat Jarernboon, and Vittaya Amornkitbamrung, Chemically deposited polypyrrole-nanoparticle counter electrode for inorganic I^-/I_3^- and organic T^-/T_2 dye-sensitized solar cells, Synthetic metals, 162 (2012) 1954-1960.
2. Wasan Maiaugree, **Samuk Pimanpang**, Madsakorn Towannang, Phikun Rutphonsan, Sekson Lowpa, Wirat Jarernboon and Vittaya Amornkitbamrung, Co-electrophoretic deposition MWCNTs/Pt counter electrodes for dye-sensitized solar cell, Japanese Journal of Applied Physics, 51 (2012) 10NE20-10NE20-6.
3. Sumeth Siriroj, **Samuk Pimanpang**, Madsakorn Towannang, Wasan Maiaugree, Santi Phumying, Wirat Jarernboon and Vittaya Amornkitbamrung, High performance dye-sensitized solar cell based on hydrothermally deposited multiwall carbon nanotube counter electrode, Applied Physics Letters, 100 (2012) 243303.
4. Wasan Maiaugree, **Samuk Pimanpang**, Madsakorn Towannang, Saman Saekow, Wirat Jarernboon and Vittaya Amornkitbamrung, Optimization of TiO2 nanoparticle mixed PEDOT–PSS counter electrodes for high efficiency dye sensitized solar cell, Journal of Non-Crystalline Solids, 358 (2012) 2489–2495.
5. Khamsone Keothongkham, **Samuk Pimanpang**, Wasan Maiaugree, Saman Saekow, Wirat Jarernboon and Vittaya Amornkitbamrung, "Electrochemically deposited polypyrrole for dye-sensitized solar cell counter electrodes" International Journal of Photoenergy, doi:10.1155/2012/671326, 2012.

Under review:

1. **Samuk Pimanpang**, Madsakorn Towannang, Anongnad Thiangkaew, Wasan Maiaugree, Pikaned Uppachai, Wirat Jarernboon and Vittaya Amornkitbamrung, "A Flexible Plastic-Stainless Steel Dye-Sensitized Solar Cell Based on Organic T^-/T_2 Electrolyte" **International Journal of Energy Research, Under reviewed, 2013.**
2. Madsakorn Towannang, Anongnad Thiangkaew, Wasan Maiaugree, Phikun Ratphonsan, Wirat Jarernboon, **Samuk Pimanpang** and Vittaya Amornkitbamrung "Thermally deposited Palladium-Tungsten Carbide and Platinum-Tungsten Carbide Counter Electrodes for High Performance Dye-Sensitized Solar Cell Based on Organic T^-/T_2 Electrolyte", **International Journal of Nanotechnology, Under reviewed, 2013.**